~~Stereolithography (SLA) 3D printing of an antihypertensive polyprintlet: Case study of an unexpected photopolymer-drug reaction~~Stereolithography (SLA) 3D printing of an antihypertensive polyprintlet: Case study of an unexpected photopolymer-drug reaction

~~Xiaoyan Xu[1], Pamela Robles-Martinez[1], Christine M. Madla[1], Fanny Joubert[1], Alvaro Goyanes[2,3,*], Abdul W. Basit[1,2,*], and Simon Gaisford[1,2,*]~~

~~[1]Department of Pharmaceutics, UCL School of Pharmacy, University College London, 29 – 39 Brunswick Square, London, WC1N 1AX, UK~~

~~[2]FabRx Ltd., 3 Romney Road, Ashford, Kent TN24 0RW, UK~~

~~[3]Departamento de Farmacología, Farmacia y Tecnología Farmacéutica, R+D Pharma Group (GI-1645), Universidade de Santiago de Compostela, 15782, Spain~~

Xiaoyan Xu[a], Pamela Robles-Martinez[a], Christine M. Madla[a], Fanny Joubert[a], Alvaro Goyanes[b,c,*], Abdul W. Basit[a,b,**], Simon Gaisford[a,b,**]

[a] Department of Pharmaceutics, UCL School of Pharmacy, University College London, 29 – 39 Brunswick Square, London, WC1N 1AX, UK

[b] FabRx Ltd., 3 Romney Road, Ashford, Kent, TN24 0RW, UK

[c] Departamento de Farmacología, Farmacia y Tecnología Farmacéutica, R+D Pharma Group (GI-1645), Universidade de Santiago de Compostela, 15782, Spain

*Correspondence: Alvaro Goyanes - a.goyanes@FabRx.co.uk

Abdul Basit – a.basit@ucl.ac.uk

Simon Gaisford - s.gaisford @ucl.ac.uk

Formatted: Superscript
Formatted: Superscript
Formatted: Superscript
Formatted: Superscript
Formatted: Superscript
Formatted: Superscript
Formatted: Superscript
Formatted: Superscript
Formatted: Superscript
Formatted: Superscript

Abstract

~~The introduction of three-dimensional (3D) printing in the pharmaceutical arena has caused a major shift towards the advancement of modern medicines, including drug products with different configurations and complex geometries. Otherwise challenging to create via conventional pharmaceutical techniques, 3D printing technologies have been explored for the fabrication of multi-drug loaded dosage forms to reduce pill burden and improve patient adherence. In this study, stereolithography (SLA), a vat polymerisation technique, was used to manufacture a multi-layer 3D printed oral dosage form (polyprintlet) incorporating four antihypertensive drugs including irbesartan, atenolol, hydrochlorothiazide and amlodipine. Although successful in its fabrication, for the first time, we report an unexpected chemical reaction between a photopolymer and drug. Fourier Transform Infrared (FTIR) spectroscopy and Nuclear Magnetic Resonance (NMR) spectroscopy confirmed the occurrence of a Michael addition reaction between the diacrylate group of the photoreactive monomer and the primary amine group of amlodipine. The study herein demonstrates the importance of careful selection of photocurable resins for the manufacture of drug-loaded oral dosage forms via SLA 3D printing technology.~~

The introduction of three-dimensional (3D) printing in the pharmaceutical arena has caused a major shift towards the advancement of modern medicines, including drug products with different configurations and complex geometries. Otherwise challenging to create via conventional pharmaceutical techniques, 3D printing technologies have been explored for the fabrication of multi-drug loaded dosage forms to reduce pill burden and improve patient adherence. In this study, stereolithography (SLA), a vat polymerisation technique, was used to manufacture a multi-layer 3D printed oral dosage form (polyprintlet) incorporating four antihypertensive drugs including irbesartan, atenolol, hydrochlorothiazide and amlodipine. Although successful in its fabrication, for the first time, we report an unexpected chemical reaction between a photopolymer and drug. Fourier Transform Infrared (FTIR) spectroscopy and Nuclear Magnetic Resonance (NMR) spectroscopy confirmed the occurrence of a Michael addition reaction between the diacrylate group of the photoreactive monomer and the primary

Formatted: Font: (Default) Arial, 11 pt

Formatted: Line spacing: 1.5 lines

Formatted: Font: (Default) Arial, 11 pt

Formatted: Font: (Default) Arial, 11 pt

Formatted: Font: (Default) Arial, 11 pt

Formatted: Font: (Default) Arial, 11 pt

Formatted: Font: (Default) Arial, 11 pt

Formatted: Font: (Default) Arial, 11 pt

Formatted: Font: (Default) Arial, 11 pt

Formatted: Font: (Default) Arial, 11 pt

Formatted: Font: (Default) Arial, 11 pt

amine group of amlodipine. The study herein demonstrates the importance of careful selection of photocurable resins for the manufacture of drug-loaded oral dosage forms via SLA 3D printing technology.

Keywords

Stereolithographic fabrication; Printing pharmaceuticals; Polypills; Fixed-dose combinations; Personalized medicines; 3D printed formulations; Polyprintlets

Formatted: Font: (Default) Arial, 11 pt

Formatted: Font: (Default) Arial, 11 pt

Formatted: English (United States)

Formatted: Add space between paragraphs of the same style, Line spacing: single, Don't adjust space between Latin and Asian text, Don't adjust space between Asian text and numbers

1. Introduction

~~Three-dimensional (3D) printing is forecasted to be a disruptive manufacturing technique from its ability to fabricate bespoke objects of virtually any shape and size in a layer-by-layer manner. Structures can be created from a digital 3D file using computer-aided design (CAD) software or imaging techniques to manufacture individualised entities on-demand [1]. 3D printing technologies have transformed a boundless field of applications including the aerospace industry [2], food sciences [3], robotics [4] and tissue and organ modelling [5] since its introduction.~~

Three-dimensional (3D) printing is forecasted to be a disruptive manufacturing technique from its ability to fabricate bespoke objects of virtually any shape and size in a layer-by-layer manner. Structures can be created from a digital 3D file using computer-aided design (CAD) software or imaging techniques to manufacture individualised entities on-demand [1]. 3D printing technologies have transformed a boundless field of applications including the aerospace industry [2], food sciences [3], robotics [4] and tissue and organ modelling [5] since its introduction.

~~From its advent in the pharmaceutical arena, 3D printing has already caused a paradigm shift in medicine manufacture. In 2016, the Food and Drug Administration (FDA) approved the first 3D printed tablet, Spritam®, which exploited the advantages of the 3D printing binder jet technique to produce orodispersible tablets for the treatment of epilepsy [1]. 3D printing technologies can be used to fabricate advanced oral dosage forms including orally disintegrating tablets [2], formulations with different geometries and size [3-5], and innovative structures [6-8] complemented with unique functions [9-15] which are otherwise challenging or near impossible to manufacture with conventional pharmaceutical techniques. Moreover, the fabrication of oral dosage forms by 3D printing allows the inclusion of multiple drug compounds in a single oral product with different configurations, such as the duoCaplet [16] or miniprintlets where doses and drug release profiles can be specifically tailored [17].~~

From its advent in the pharmaceutical arena, 3D printing has already caused a paradigm shift

Formatted: Font: (Default) Arial, 11 pt

Formatted: Font: (Default) Arial, 11 pt

Formatted: Font: (Default) Arial, 11 pt

Formatted: Font: (Default) Arial, 11 pt

Formatted: Font: (Default) Arial, 11 pt

Formatted: Font: (Default) Arial, 11 pt

Formatted: English (United States)

in medicine manufacture. In 2016, the Food and Drug Administration (FDA) approved the first 3D printed tablet, Spritam®, which exploited the advantages of the 3D printing binder jet technique to produce orodispersible tablets for the treatment of epilepsy [6]. 3D printing technologies can be used to fabricate advanced oral dosage forms including orally disintegrating tablets [7], formulations with different geometries and size [8–10], and innovative structures [11–13] complemented with unique functions [14–20] which are otherwise challenging or near impossible to manufacture with conventional pharmaceutical techniques. Moreover, the fabrication of oral dosage forms by 3D printing allows the inclusion of multiple drug compounds in a single oral product with different configurations, such as the duoCaplet [21] or miniprintlets where doses and drug release profiles can be specifically tailored [22].

~~Several 3D printing technologies have proved their amenability in the pharmaceutical field, including fused deposition modelling (FDM), selective laser sintering (SLS), binder jetting and semi-solid extrusion [1]. Vat photopolymerisation techniques such as stereolithography (SLA) [2], digital light processing (DLP) [3] and continuous liquid interface production (CLIP) [4] are processes that utilise light irradiation (e.g. laser beam, UV and visible light) to create solid objects from a photoreactive liquid resin. Such methods offer several advantages including great feature resolution, a smooth surface finish and avoidance of drug thermal degradation [5, 6]. Generally, there are two main photopolymerisation systems including i) free radical and ii) ionic reactions. In both mechanisms, a photoinitiator system is responsible to generate reactive species (free radical, cations or anions) in order to initiate photopolymerisation [7]. Methacrylate-based and acrylate-based monomers are most widely used in the free radical system, demonstrating fast reaction rates and tunable mechanical properties [8]. Free radical photopolymerisation is an attractive and versatile platform for the development of pharmaceutical products as the active components can simply be blended with photocurable monomers prior to printing and become trapped in the polymeric cross-linked network. Previously, controlled release drug loaded hydrogels were successfully prepared using poly(ethylene glycol) diacrylate as the main photocurable monomers and riboflavin as a non-~~

Formatted: English (United States)

~~toxic photoinitiator via SLA 3D printing [9]. SLA technology has also demonstrated its success in the fabrication of a single oral dosage forms incorporating up to six drugs [10].~~

Several 3D printing technologies have proved their amenability in the pharmaceutical field, including fused deposition modelling (FDM), selective laser sintering (SLS), binder jetting and semi-solid extrusion [23]. Vat photopolymerisation techniques such as stereolithography (SLA) [24], digital light processing (DLP) [25] and continuous liquid interface production (CLIP) [26] are processes that utilise light irradiation (e.g. laser beam, UV and visible light) to create solid objects from a photoreactive liquid resin. Such methods offer several advantages including great feature resolution, a smooth surface finish and avoidance of drug thermal degradation [27,28]. Generally, there are two main photopolymerisation systems including i) free radical and ii) ionic reactions. In both mechanisms, a photoinitiator system is responsible to generate reactive species (free radical, cations or anions) in order to initiate photopolymerisation [29]. Methacrylate- and acrylate-based monomers are most widely used in the free radical system, demonstrating fast reaction rates and tunable mechanical properties [30]. Free radical photopolymerisation is an attractive and versatile platform for the development of pharmaceutical products as the active components can simply be blended with photocurable monomers prior to printing and become trapped in the polymeric cross-linked network. Previously, controlled-release drug-loaded hydrogels were successfully prepared using poly(ethylene glycol) diacrylate as the main photocurable monomers and riboflavin as a non-toxic photoinitiator via SLA 3D printing [31]. SLA technology has also demonstrated its success in the fabrication of a single oral dosage forms incorporating up to six drugs [32].

Combination therapy has gained momentum with the aim of improving therapeutic outcomes currently achieved by polypharmacy. The concurrent use of multiple medications by a patient, however, is an ongoing concern due to the high pill burden, patient non-adherence and increasing risk of medication errors [33,34]. To overcome such limitations, “polypills”, the concept of incorporating more than one active pharmaceutical ingredient in a single dosage

form, was devised as an optimised therapeutic approach for treatments such as cardiovascular disease (CVD) [35]. Recently, a high-impact clinical study investigated the therapeutic outcome of a single polypill containing four antihypertensive drugs [36] (atenolol, hydrochlorothiazide, irbesartan and amlodipine) and demonstrated that a single polypill achieved a greater reduction in high blood pressure when compared with the standard dose of each medication alone.

This study aimed to explore the amenability of SLA 3D printing to fabricate a multi-layer antihypertensive polypill (herein coined as a polyprintlet) of four antihypertensive drugs (irbesartan, atenolol, hydrochlorothiazide and amlodipine) with a secondary aim to study the unexpected chemical reaction between the photopolymers and drugs.

Formatted: English (United States)

~~Combination therapy has gained momentum with the aim of improving therapeutic outcomes currently achieved by polypharmacy. The concurrent use of multiple medications by a patient, however, is an ongoing concern due to the high pill burden, patient non-adherence and increasing risk of medication errors [1, 2]. To overcome such limitations, "polypills", the concept of incorporating more than one active pharmaceutical ingredient in a single dosage form, was devised as an optimised therapeutic approach for treatments such as cardiovascular disease (CVD) [3]. Recently, a high-impact clinical study investigated the therapeutic outcome of a single polypill containing four antihypertensive drugs [4] (atenolol, hydrochlorothiazide, irbesartan and amlodipine) and demonstrated that a single polypill achieved a greater reduction in high blood pressure when compared with the standard dose of each medication alone.~~

~~This study aimed to explore the amenability of SLA 3DP to fabricate a multi-layer antihypertensive polypill (herein coined as a polyprintlet) of four antihypertensive drugs (irbesartan, atenolol, hydrochlorothiazide and amlodipine) with a secondary aim to study the unexpected chemical reaction between the photopolymers and drugs.~~

2. Materials and mMethods

2.1 Materials

~~Hydrochlorothiazide (MW 297.74 g/mol), poly(ethylene glycol) diacrylate (PEGDA, average M„ 575 g/mol) and diphenyl(2, 4, 6-trimethyl benzoyl) phosphine oxide (TPO) were purchased from Sigma-Aldrich, UK. Irbesartan (MW 428.53 g/mol) was obtained from Sun Pharmaceutical Industries Ltd., India. Amlodipine (MW 408.88 g/mol) and atenolol (MW 266.34 g/mol) were purchased from LKT Laboratories Inc., USA. Poly(ethylene glycol) (PEG 300, average MW 300 g/mol) was acquired from Acros Organics, UK.~~

~~Acetonitrile (ACN, ≥99.9%, HPLC grade) was supplied by Sigma-Aldrich, UK. Formic acid (FA, Optima, LC-MS grade) was purchased from Fisher Scientific, UK. The salts for the preparation of the buffer dissolution media were purchased from VWR International Ltd., UK. Dimethyl sulfoxide-d6 (99.9%) was obtained from Cambridge Isotope Laboratories, Inc., USA.~~

Hydrochlorothiazide (MW 297.74 g/mol), poly(ethylene glycol) diacrylate (PEGDA, average Mn 575 g/mol) and diphenyl(2, 4, 6-trimethyl- benzoyl) phosphine oxide (TPO) were purchased from Sigma- Aldrich, UK. Irbesartan (MW 428.53 g/mol) was obtained from Sun Pharmaceutical Industries Ltd., India. Amlodipine (MW 408.88 g/mol) and atenolol (MW 266.34 g/mol) were purchased from LKT Laboratories Inc., USA. Poly(ethylene glycol) (PEG 300, average MW 300 g/mol) was acquired from Acros Organics, UK.

Acetonitrile (ACN, ≥ 99.9 %, HPLC grade) was supplied by Sigma-Aldrich, UK. Formic acid (FA, Optima, LC–MS grade) was purchased from Fisher Scientific, UK. The salts for the preparation of the buffer dissolution media were purchased from VWR International Ltd., UK. Dimethyl sulfoxide-d6 (99.9 %) was obtained from Cambridge Isotope Laboratories, Inc., USA.

Formatted: English (United States)

2.2. Design of the polyprintlets

~~Four drugs were incorporated in different regions of the polyprintlet (Figure 1) and explored in~~

~~two orientations; Type 1 and Type 2. The selected dimensions of the polyprintlet was 10 mm diameter × 5 mm height with a 1 mm layer thickness for each drug, except for irbesartan. Irbesartan was designed to be2 mm in thickness. The thickness of irbesartan layer was doubled (2mm) to allow a lower concentration of drug in the layer (20.9% w/w) to obtain the desired dose (Table 1). . If the thickness of irbesartan layer was 1mm the required drug concentration would be 41.8% w/w, which is not printable. The Type 1 polyprintlet was designed to incorporate the drugs with higher doses (irbesartan and atenolol) on the outer layers and lower dosed drugs (hydrochlorothiazide and amlodipine) in the inner layers (Table 1). The order of drugs in the Type 2 polyprintlet was changed.~~ Four drugs were incorporated in different regions of the polyprintlet (Fig. 1) and explored in two orientations; Type 1 and Type 2. The selected dimensions of the polyprintlet was 10mm diameter × 5mm height with a 1mm layer thickness for each drug, except for irbesartan. The thickness of irbesartan layer was doubled (2 mm) to allow a lower concentration of drug in the layer (20.9 % w/w) to obtain the desired dose (Table 1). If the thickness of irbesartan layer was 1mm the required drug concentration would be 41.8 % w/w, which is not printable. The Type 1 polyprintlet was designed to incorporate the drugs with higher doses (irbesartan and atenolol) on the outer layers and lower dosed drugs (hydrochlorothiazide and amlodipine) in the inner layers (Table 1). The order of the drugs in the Type 2 polyprintlet was changed to have the following arrangement; amplodipine and hydrochlorothiazide on the outer layers and irbesartan and atenolol in the inner layers.

Formatted: English (United States)

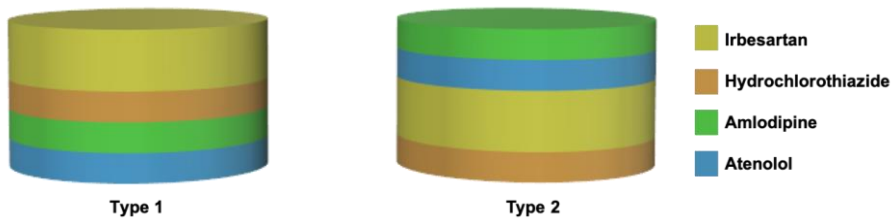

Fig.~~ure~~ 1. 3D designs of the polyprintlets (10 mm diameter and 5 mm height).

2.3 Preparation of photopolymer solutions

The photopolymer solutions were prepared with 1% (w/w) of diphenyl(2, 4, 6-trimethyl-benzoyl) phosphine oxide (TPO) added to a total mass of 5 g. The pure drugs were added to each solution according to previously calculated concentrations (Table 1). PEG 300 was added as a diluent to decrease the crosslinking density at a ratio of 35% (w/w) PEGDA to 65% (w/w) PEG 300. The photopolymer solutions were mixed thoroughly for 3 h at room temperature until the drugs and photoinitiator were fully dissolved in the photopolymer solutions.

Table 1. Amount of material used for each layer in a 5 g solution preparation

Layer	Drug (g)	PEG 300 (g)	PEGDA (g)
Irbesartan	1.04 (20.9 % w/w)	2.54 (50.8 % w/w)	1.37 (27.4 % w/w)
Atenolol	0.70 (13.9 % w/w)	2.77 (55.3 % w/w)	1.49 (29.8 % w/w)
Hydrochlorothiazide	0.35 (6.9 % w/w)	2.99 (59.8 % w/w)	1.61 (32.2 % w/w)
Amlodipine	0.07 (1.4 % w/w)	3.17 (63.5 % w/w)	1.71 (34.2 % w/w)

*each formulation included 1 % (w/w) TPO.

Formatted Table
Formatted: Left
Formatted: Left
Formatted: Left
Formatted: Left
Formatted: Left

2.4 Printing process

~~The photopolymer solution was loaded into a commercial Form 1+ SLA 3D printer (Formlabs Inc., USA) equipped with a 405 nm laser. The geometry of the polyprintlet was designed with AutoCAD 2015 (Autodesk Inc., USA) and exported as a stereolithography file (.stl) in the 3D printer software (Preform Software v. 2.3.3 OpenFL, Formlabs, USA). The Form 1+ SLA 3D printer is designed to print uniform objects with only one material. In order to allow the use of different materials in a single object, the operation of the printer was conducted using OpenFL. This application programming interface was developed by FormLabs for the Form 1 and Form 1+ SLA 3D printers and has previously been described in the literature [1]. The OpenFL software allows the user to pause the printing process and raise the build platform in order to change the material on the resin tray. After changing the material, the build platform was lowered to its previous position and printing was resumed. Deionised water was used to rinse~~

~~the printed layer between materials to avoid cross contamination. In the material print setting, the customised number of laser passes was selected as 10 for the first layer and 2 for the remaining layers with a layer thickness of 100 µm to achieve high resolution. The polyprintlets were printed directly on the platform without the need of any support.~~

The photopolymer solution was loaded into a commercial Form 1+SLA 3D printer (Formlabs Inc., USA) equipped with a 405 nm laser. The geometry of the polyprintlet was designed with AutoCAD 2015 (Autodesk Inc., USA) and exported as a stereolithography file (.stl) in the 3D printer software (Preform Software v. 2.3.3 OpenFL, Formlabs, USA). The Form 1+SLA 3D printer is designed to print uniform objects with only one material. In order to allow the use of different materials in a single object, the operation of the printer was conducted using OpenFL. This application programming interface was developed by FormLabs for the Form 1 and Form 1+SLA 3D printers and has previously been described in the literature [32]. The OpenFL software allows the user to pause the printing process and raise the build platform in order to change the material on the resin tray. After changing the material, the build platform was lowered to its previous position and printing was resumed. Deionised water was used to rinse the printed layer between materials to avoid cross contamination. In the material print setting, the customised number of laser passes was selected as 10 for the first layer and 2 for the remaining layers with a layer thickness of 100 µm to achieve high resolution. The polyprintlets were printed directly on the platform without the need of any support.

Formatted: English (United States)

2.5 Polyprintlet dimensions

The polyprintlets were weighed and measured (width and height) in triplicate using a digital calliper (0.150 mm PRO-MAX, Fowler, mod S 235 PAT).

2.6 Scanning ~~E~~electron ~~M~~icroscopy (SEM)

The polyprintlet samples were previously cut in half and attached to a self-adhesive carbon disc mounted on a 25 mm aluminium stub, which was coated with 25 nm of gold using a sputter coater. The stub was then placed into a FEI Quanta 200 FEG Scanning Electron Microscope

(FEI, UK) at 5 kV accelerating voltage using secondary electron detection to obtain the cross-section images of the SLA 3D printed polyprintlets.

2.7 X-ray pPowder dDiffraction (XRPD)

~~Single drug-loaded discs (23 mm diameter × 1 mm height) and discs without drugs (control) were printed via SLA and analysed together with the four drugs individually. X-ray powder diffraction patterns were obtained in a Rigaku MiniFlex 600 (Rigaku, USA) using a Cu Kα X-ray source (λ=1.5418Å). The angular range of data acquisition was 3-60° 2θ with a stepwise size of 0.02° at a speed of 5°/min. The intensity and voltage applied were 15 mA and 40 kV.~~

–Single drug-loaded discs (23mm diameter × 1mm height) and discs without drugs (control) were printed via SLA and analysed together with the four drugs individually. X-ray powder diffraction patterns were obtained in a Rigaku MiniFlex 600 (Rigaku, USA) using a Cu K α X-ray source (λ =1.5418 Å). The angular range of data acquisition was 3–60° 2 θ with a stepwise size of 0.02° at a speed of 5°/min. The intensity and voltage applied were 15 mA and 40 kV.

2.8 Thermal analysis

Differential scanning calorimetry (DSC) was used to characterise the single drug-loaded 3D printed formulations, the control and the pure drug samples. DSC measurements were performed with a Q2000 DSC (TA instruments, Waters, LLC, USA) at a heating rate of 10 °C/min. Calibrations for cell constant and enthalpy were performed with indium (Tm=156.6 °C, Δ Hf=28.71 J/g) according to the manufacturer instructions. Nitrogen was used as a purge gas with a flow rate of 50 mL/min for all the experiments. Data were collected with TA Advantage software for Q series (version 2.8.394) and analysed using TA Instruments Universal Analysis 2000. All melting temperatures are reported as extrapolated onset unless otherwise stated. TA aluminium pans and pin-holed hermetic lids (Tzero) were used with an average sample mass of 8–10 mg.~~Differential scanning calorimetry (DSC) was used to characterise the single drug-loaded 3D printed formulations, the control and the pure drug samples. DSC measurements were performed with a Q2000 DSC (TA instruments, Waters,~~

~~LLC, USA) at a heating rate of 10ºC/min. Calibrations for cell constant and enthalpy were performed with indium (T_m = 156.6ºC, ΔH_f = 28.71 J/g) according to the manufacturer instructions. Nitrogen was used as a purge gas with a flow rate of 50 mL/min for all the experiments. Data were collected with TA Advantage software for Q series (version 2.8.394) and analysed using TA Instruments Universal Analysis 2000. All melting temperatures are reported as extrapolated onset unless otherwise stated. TA aluminium pans and pin holed hermetic lids (T_{zero}) were used with an average sample mass of 8 – 10 mg.~~

2.9 Determination of drug content in the photopolymer resins and 3DP polyprintlets

~~To quantify the drug content of the resins, aliquots of each photopolymer solution loaded with drug were weighed and diluted together with 70% (v/v) methanol and 30% (v/v) water in volumetric flasks (10 mL). The solutions were left under magnetic stirring overnight and filtered through 0.45 µm filter (Merck Millipore Ltd., Ireland). The concentration of drug was then determined by HPLC (Agilent 1260 Infinity Quaternary LC System).~~

~~For determination of drug loading in the polyprintlet, single drug-loaded layers were crushed and dissolved together with 70% (v/v) methanol and 30% (v/v) water in volumetric flasks (25 mL). Samples of the solutions were left under magnetic stirring overnight then filtered through 0.45 µm syringe filter (Merck Millipore Ltd., Ireland) and the concentration of drug was determined by HPLC.~~

~~The gradient mobile phase consisted of (A) 0.1% v/v FA in water, (B) methanol and (C) ACN which was pumped at a flowrate of 1 mL/min through a Luna 5u Phenyl-Hexyl 5 µm column, 250 mm × 4.6 mm (Phenomenex) under the gradient program shown in Table 2. The sample injection volume was 30 µL and the total run time was 13 min, operating at room temperature at a wavelength of 215 nm.~~

To quantify the drug content of the resins, aliquots of each photopolymer solution loaded with drug were weighed and diluted together with 70 % (v/v) methanol and 30 % (v/v) water in

volumetric flasks (10 mL). The solutions were left under magnetic stirring overnight and filtered through 0.45 µm filter (Merck Millipore Ltd., Ireland). The concentration of drug was then determined by HPLC (Agilent 1260 Infinity Quaternary LC System).

For determination of drug loading in the polyprintlet, single drug-loaded layers were crushed and dissolved together with 70 % (v/v) methanol and 30 % (v/v) water in volumetric flasks (25 mL). Samples of the solutions were left under magnetic stirring overnight then filtered through 0.45 µm syringe filter (Merck Millipore Ltd., Ireland) and the concentration of drug was determined by HPLC.

The gradient mobile phase consisted of (A) 0.1 % v/v FA in water, (B) methanol and (C) ACN which was pumped at a flowrate of 1 mL/min through a Luna 5 u Phenyl-Hexyl 5 µm column, 250mm × 4.6mm (Phenomenex) under the gradient program shown in Table 2. The sample injection volume was 30 µL and the total run time was 13 min, operating at room temperature at a wavelength of 215 nm.

Table 2. Gradient programme for the mobile phase.

Time (min)	0.1% FA in water (% A)	Methanol (% B)	ACN (% C)
0.0	95	0	5
5.5 – **6**.0	50	0	50
6.5	87	0	13
9.0 – **10**.0	77	10	13
11.0	95	0	5

2.10 Fourier-Transform iInfrared spectroscopy (FTIR)

~~The infrared spectra were collected using a Spectrum 100 FTIR spectrometer (PerkinElmer, Waltham, MA). Pure amlodipine drug powder and PEGDA were measured as the references. Physical mixtures containing 1.39%, 10%, 20%, 30% and 50% (w/w) of amlodipine in PEGDA~~

Formatted: Justified
Formatted Table
Formatted: Left
Formatted: Left
Formatted: Left
Formatted: Left
Formatted: Left
Formatted: Left

~~were prepared by thoroughly stirring. All samples were scanned over a range of 4000 – 650cm^{-1} at a resolution of 1 cm^{-1} for 64 scans.~~ The infrared spectra were collected using a Spectrum 100 FTIR spectrometer (PerkinElmer, Waltham, MA). Pure amlodipine drug powder and PEGDA were measured as the references. Physical mixtures containing 1.39 %, 10 %, 20 %, 30 % and 50 % (w/w) of amlodipine in PEGDA were prepared by thoroughly stirring. All samples were scanned over a range of 4000 – 650 cm−1 at a resolution of 1 cm−1 for 64 scans.

2.11 Nuclear m~~M~~agnetic r~~R~~esonance (NMR) spectroscopy

~~All NMR spectra were recorded in 99.9% DMSO-d6 (Cambridge Isotope Laboratories, Inc., USA).^{1}H NMR spectra of amlodipine and PEGDA were obtained separately. In order to investigate the reaction between amlodipine and PEGDA, sample solution of amlodipine mixed with PEGDA (molar ratio of 2:1) was prepared. ^{1}H and ^{13}C NMR spectra of the solutions were obtained using a Bruker AVANCE 400 spectrometer. Data acquisition and processing were performed using standard TopSpin software (Bruker, UK).~~All NMR spectra were recorded in 99.9 % DMSO-d6 (Cambridge Isotope Laboratories, Inc., USA).1H-NMR spectra of amlodipine and PEGDA were obtained separately. In order to investigate the reaction between amlodipine and PEGDA, sample solution of amlodipine mixed with PEGDA (molar ratio of 2:1) was prepared. 1H and 13C NMR spectra of the solutions were obtained using a Bruker AVANCE 400 spectrometer. Data acquisition and processing were performed using standard TopSpin software (Bruker, UK).

2.12 Dissolution testing conditions

Dissolution profiles for each 3D printed polyprintlet were obtained using USP-II apparatus (Model PTWS, Pharmatest, Germany). Polyprintlets were first placed in 750 mL of 0.1M HCl for 2 h to simulate gastric residence time and then transferred into 950 mL of physiological bicarbonate buffer (Hanks buffer) (pH 5.6–7) for 35 min followed by 1000 mL of modified Krebs buffer (pH 7–7.4 and then to 6.5). Hanks buffer (0.441 mM KH_2PO_4, 0.337 mM Na_2HPO_4 ·

Formatted: Subscript
Formatted: Subscript
Formatted: Subscript
Formatted: Subscript

$2H_2O$, 136.9 mM NaCl, 5.37 mM KCl, 0.812 mM $MgSO_4 \cdot 7H_2O$, 1.26 mM $CaCl_2 \cdot 2H_2O$, 4.17 mM $NaHCO_3$) was modified to form an in-situ modified Kreb's buffer by the addition of 50 mL of pre-Krebs solution (6.9 mM KH_2PO_4 and 400.7 mM $NaHCO_3$) to every dissolution vessel [37,38].

The polyprintlets were tested in small intestinal environment for 3.5 h with the pH value of 5.6–7.4, followed by pH 6.5 representing the colonic environment [37,38]. The dissolution medium is primarily a bicarbonate buffer system in which both bicarbonate (HCO_3^-) and carbonic acid (H_2CO_3) exist in an equilibrium together with CO_2 (aq) resulting from the dissociation of the carbonic acid [38]. The pH of the bicarbonate buffer is modulated and controlled by an Auto pH System™ which incorporates a pH probe connected to a supply of CO_2 (pH reducing gas), as well as to a supply of helium (pH increasing gas) [39]. During dissolution testing, the control unit monitors the pH changes and adjusts the pH by feeding CO_2 or helium into the dissolution vessel. The paddle speed of the USP-II was fixed at 50 rpm and the dissolution media was maintained at 37 ± 0.5 °C. 1 mL samples of the dissolution media were withdrawn every half an hour in the first 3 h, followed by every hour. The concentration of the drugs was determined by HPLC (previously described in section 2.9) to calculate the percentage of drug released from the polyprintlets. ~~Dissolution profiles for each 3D printed polyprintlet were obtained using USP-II apparatus (Model PTWS, Pharmatest, Germany). Polyprintlets were first placed in 750 mL of 0.1 M HCl for 2 h to simulate gastric residence time and then transferred into 950 mL of physiological bicarbonate buffer (Hanks buffer) (pH 5.6 to 7) for 35 min followed by 1000 mL of modified Krebs buffer (pH 7 to 7.4 and then to 6.5). Hanks buffer (0.441 mM KH_2PO_4, 0.337 mM $Na_2HPO_4 \cdot 2H_2O$, 136.9 mM NaCl, 5.37 mM KCl, 0.812 mM $MgSO_4 \cdot 7H_2O$, 1.26 mM $CaCl_2 \cdot 2H_2O$, 4.17 mM $NaHCO_3$) was modified to form an in-situ modified Kreb's buffer by the addition of 50 mL of pre-Krebs solution (6.9 mM KH_2PO_4 and 400.7 mM $NaHCO_3$) to every dissolution vessel [1, 2].~~

Formatted: Subscript
Formatted: Subscript
Formatted: Subscript
Formatted: Subscript
Formatted: Subscript
Formatted: Subscript
Formatted: Subscript
Formatted: Subscript
Formatted: Subscript
Formatted: Subscript
Formatted: Superscript
Formatted: Subscript
Formatted: Subscript
Formatted: Subscript
Formatted: Subscript

~~The polyprintlets were tested in small intestinal environment for 3.5 h with the pH value of 5.6 to 7.4, followed by pH 6.5 representing the colonic environment [1, 2]. The dissolution medium is primarily a bicarbonate buffer system in which both bicarbonate (HCO_3^-) and carbonic acid (H_2CO_3) exist in an equilibrium together with CO_2 (aq) resulting from the dissociation of the carbonic acid [2]. The pH of the bicarbonate buffer is modulated and controlled by an Auto pH System™ which incorporates a pH probe connected to a supply of CO_2 (pH reducing gas), as well as to a supply of helium (pH increasing gas) [3]. During dissolution testing, the control unit monitors the pH changes and adjusts the pH by feeding CO_2 or helium into the dissolution vessel. The paddle speed of the USP II was fixed at 50 rpm and the dissolution media was maintained at 37 ± 0.5ºC. 1 mL samples of the dissolution media were withdrawn every half an hour in the first 3 hours, followed by every hour. The concentration of the drugs was determined by HPLC (previously described in section 2.9) to calculate the percentage of drug released from the polyprintlets.~~

3. Results and dDiscussion

The study herein demonstrates the amenability to incorporate the selected drugs in a resin to be 3D printed via SLA. Pure amlodipine and hydrochlorothiazide readily dissolved in the photopolymer solution although a longer time was required to completely dissolve atenolol and irbesartan. Hydrochlorothiazide and amlodipine solutions were clear, although both of the printed layers appeared off-white. A white solution was achieved following the homogenous dispersion of pure atenolol in the photopolymer solution, however, after completely dissolving the atenolol solution became clear. The irbesartan suspension was creamy and viscous as it contained a high concentration of drug (20.8 % w/w).

Drug loaded polyprintlets were successfully fabricated as shown in Fig. 2.

Type 1 and 2 polyprintlets were printed with good resolution and consistency in shape. The printing settings were customised and optimised for the different formulations using the

OpenFL software. The Type 1 polyprintlet (diameter 11.2mm ± 0.3 mm, height 5.4mm ± 0.3 mm) was slightly wider in diameter but shorter in height when compared with the Type 2 polyprintlet (diameter 10.4mm ± 0.2 mm, height 6.7mm ± 0.3 mm).

~~The study herein demonstrates the amenability to incorporate the selected drugs in a resin to be 3D printed via SLA. Pure amlodipine and hydrochlorothiazide readily dissolved in the photopolymer solution although a longer time was required to completely dissolve atenolol and irbesartan. Hydrochlorothiazide and amlodipine solutions were clear, although both of the printed layers appeared off white. A white solution was achieved following the homogenous dispersion of pure atenolol in the photopolymer solution, however, after completely dissolving the atenolol solution became clear. The irbesartan suspension was creamy and viscous as it contained a high concentration of drug (20.8% w/w).~~

~~Drug loaded polyprintlets were successfully fabricated as shown in Figure 2.~~

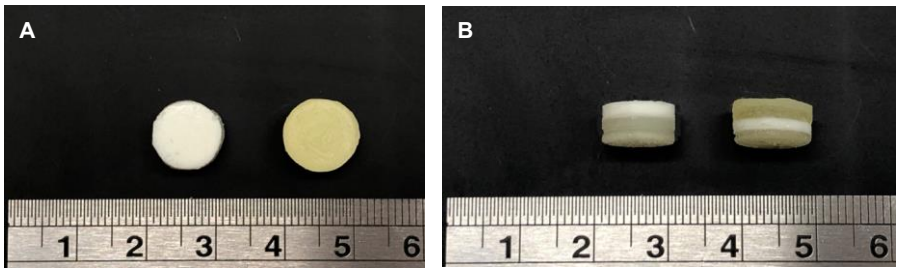

Fig~~ure~~ 2. Top view (A) and lateral view (B) of Type 1 (left) and Type 2 (right) polyprintlets. Type 1 was loaded with (from top to bottom) irbesartan, amlodipine, hydrochlorothiazide and atenolol. Type 2 was loaded with (from top to bottom) amlodipine, atenolol, irbesartan and hydrochlorothiazide. The scale is in cm.

SEM imaging was used to visualise the structures of the polyprintlets (Fig. 3). The cross section of the Type 2 polyprintlet show visible signs of separation between the four printed layers. This indicates that the individual drug and resin did not mix during the printing process.

~~Type 1 and 2 polyprintlets were printed with good resolution and consistency in shape. The printing settings were customised and optimised for the different formulations using the OpenFL software. The Type 1 polyprintlet (diameter 11.2 mm ± 0.3 mm, Height 5.4 mm ± 0.3 mm) was slightly wider in diameter but shorter in height when compared with the Type 2 polyprintlet (diameter 10.4 mm ± 0.2 mm, Height 6.7 mm ± 0.3 mm).~~

~~SEM imaging was used to visualise the structures of the polyprintlets (Figure 3). The cross section of the Type 2 polyprintlet show visible signs of separation between the four printed layers. This indicates that the individual drug and resin did not mix during the printing process.~~

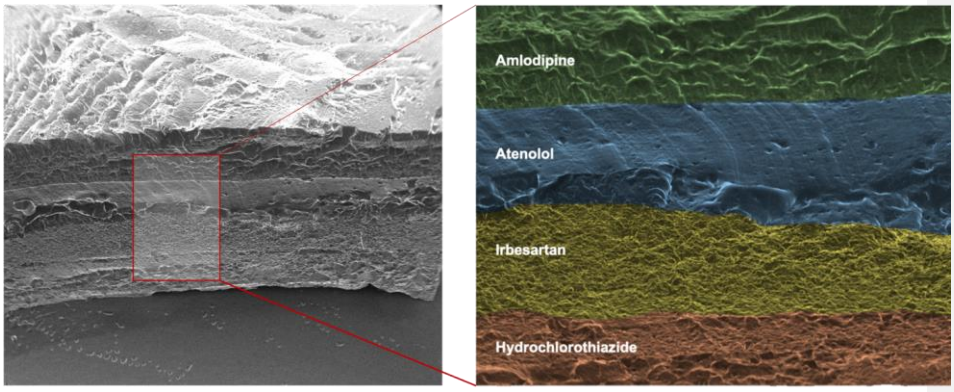

Fig~~ure~~ 3. SEM image of cross section of the Type 2 polyprintlet loaded with (from top to bottom) amlodipine, atenolol, irbesartan and hydrochlorothiazide.

Pure drug samples and SLA 3D printed discs were analysed by XRD to evaluate the incorporation of drugs in the drug-polymer matrices. The diffractogram outlines peaks of pure atenolol at around 20 ° 2 θ (Fig. 4). Peaks at 9.5 ° 2 θ, 19.5 ° 2 θ and 23.8 ° 2 θ were observed in pure amlodipine and peaks at 18.6 ° 2 θ and 28.3 ° 2 θ were shown in pure hydrochlorothiazide. The absence of these peaks in atenolol, amlodipine and hydrochlorothiazide 3D printed formulations indicated that the drugs existed in the amorphous form with the absence of crystal formation during the printing process. Conversely, typical

peaks of irbesartan at around 4.4 ° 2 θ and 12.1 ° 2 θ were still visible in the printed formulation indicating that irbesartan was existing in its partially crystalline form in the printed formulation. This suggests that the irbesartan drug powder may not have fully dissolved in the photopolymer solution prior to printing.

~~Pure drug samples and SLA 3D printed discs were analysed by XRD to evaluate the incorporation of drugs in the drug-polymer matrices. The diffractogram outlines peaks of pure atenolol at around 20° 2θ (Figure 4). Peaks at 9.5° 2θ, 19.5° 2θ and 23.8° 2θ were observed in pure amlodipine and peaks at 18.6° 2θ and 28.3° 2θ were shown in pure hydrochlorothiazide. The absence of these peaks in atenolol, amlodipine and hydrochlorothiazide 3D printed formulations indicated that the drugs existed in the amorphous form with the absence of crystal formation during the printing process. Conversely, typical peaks of irbesartan at around 4.4° 2θ and 12.1° 2θ were still visible in the printed formulation indicating that irbesartan was existing in its partially crystalline form in the printed formulation. This suggests that the irbesartan drug powder may not have fully dissolved in the photopolymer solution prior to printing.~~

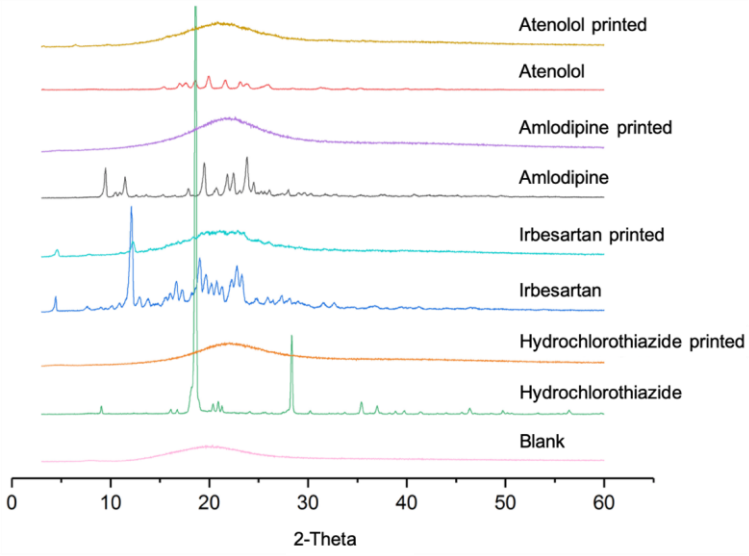

Figure 4. X-ray powder diffractograms of pure drugs and printed formulations.

DSC analysis of pure drugs and the 3D printed formulations were performed in order to determine the physical state of drugs in the photopolymer solutions before and after printing. The DSC results showed melting peaks at 154 °C, 140 °C and 273 °C for pure atenolol, amlodipine and hydrochlorothiazide respectively (Fig. 5). No evidence of melting was observed in the atenolol, amlodipine and hydrochlorothiazide 3D printed formulations which indicate that the drugs completely dissolved in the photopolymer solutions before printing which was further corroborated by the XRD findings. The DSC of pure irbesartan showed a sharp endothermic peak at around 187 °C which corresponded to the melting point of irbesartan. A small exothermic peak was also observed in the irbesartan printed formulation which suggests that the irbesartan powder was not completely dissolved in the photopolymer solution.

~~DSC analysis of pure drugs and the 3D printed formulations were performed in order to determine the physical state of drugs in the photopolymer solutions before and after printing. The DSC results showed melting peaks at 154ºC, 140º and 273ºC for pure atenolol, amlodipine and hydrochlorothiazide respectively (Figure 5). No evidence of melting was observed in the~~

~~atenolol, amlodipine and hydrochlorothiazide 3D printed formulations which indicate that the drugs completely dissolved in the photopolymer solutions before printing which was further corroborated by the XRD findings. The DSC of pure irbesartan showed a sharp endothermic peak at around 187ºC which corresponded to the melting point of irbesartan. A small exothermic peak was also observed in the irbesartan printed formulation which suggests that the irbesartan powder was not completely dissolved in the photopolymer solution.~~

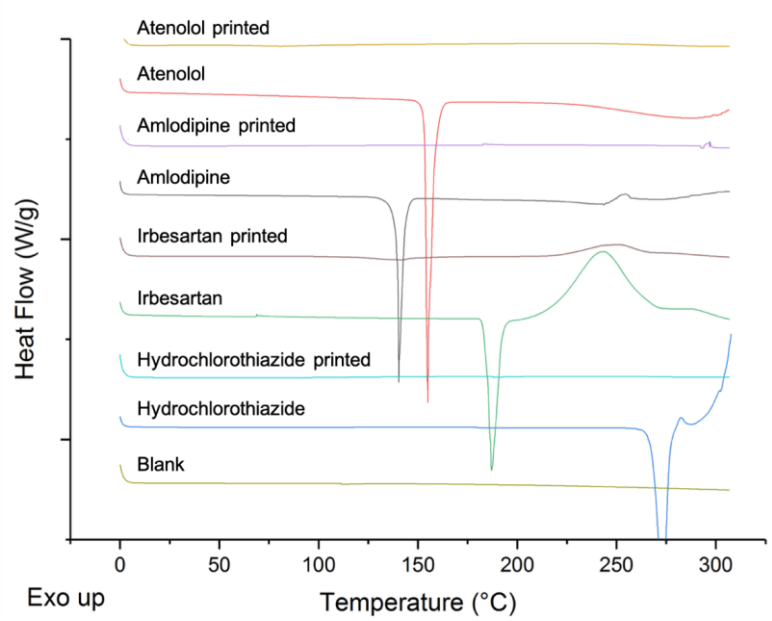

Fig~~ure~~ 5. DSC thermal traces of pure drugs and printed formulations.

Drug loading of irbesartan, atenolol and hydrochlorothiazide in the 3D printed layers were slightly lower than that in the photopolymer solution which may be due to incomplete drug extraction from the crosslinked network (Table 3). Noticeably, amlodipine was detected in neither the photopolymer solution nor the printed layer which suggests a possible reaction between amlodipine and PEGDA during the mixing process.~~Drug loading of irbesartan, atenolol and hydrochlorothiazide in the 3D printed layers were slightly lower than that in the photopolymer solution which may be due to incomplete drug extraction from the crosslinked network (Table 3). Noticeably, amlodipine was detected in neither the photopolymer solution~~

~~nor the printed layer which suggests a possible reaction between amlodipine and PEGDA during the mixing process.~~

Table 3. Drug loading in photopolymer solutions and printed individual layers.

Drug	Theoretical drug loading (%, w/w)	Drug loading in photopolymer solutions (%, w/w)	Drug loading in SLA 3D printed layers (%, w/w)
Irbesartan	20.85	20.85 ± 0.05	18.70 ± 0.82
Atenolol	13.90	13.86 ± 1.60	12.66 ± 0.39
Hydrochlorothiazide	6.95	7.10 ± 0.16	6.14 ± 0.01
Amlodipine	1.39	-	-

Formatted: Left

Formatted: Left

Formatted: Left

Formatted: Left

FTIR was firstly employed to investigate the potential cause of drug and photopolymer reaction. Different masses of amlodipine were mixed with PEGDA until the drug was fully dissolved accompanied with continuous magnetic stirring. Results from FTIR showed that the typical peak of amlodipine at 3390 cm−1 (N-H bond stretching) was not observed in any of the spectra of amlodipine-PEGDA mixtures regardless of the concentration which could indicate a possible effect on the N-H bonds of amlodipine (Fig. 6). In addition, the intensity of C]C peak of PEGDA at 1636 cm−1 decreased when the amlodipine:PEGDA ratio increased. As such, a further reaction may occur with the acrylate groups as well.~~FTIR was firstly employed to investigate the potential cause of drug and photopolymer reaction. Different masses of amlodipine were mixed with PEGDA until the drug was fully dissolved accompanied with continuous magnetic stirring. Results from FTIR showed that the typical peak of amlodipine at 3390 cm^{-1} (N-H bond stretching) was not observed in any of the spectra of amlodipine-PEGDA mixtures regardless of the concentration which could indicate a possible effect on the N-H bonds of amlodipine (Figure 6). In addition, the intensity of C=C peak of PEGDA at 1636 cm^{-1} decreased when the~~

~~amlodipine:PEGDA ratio increased. As such, a further reaction may occur with the acrylate groups as well.~~

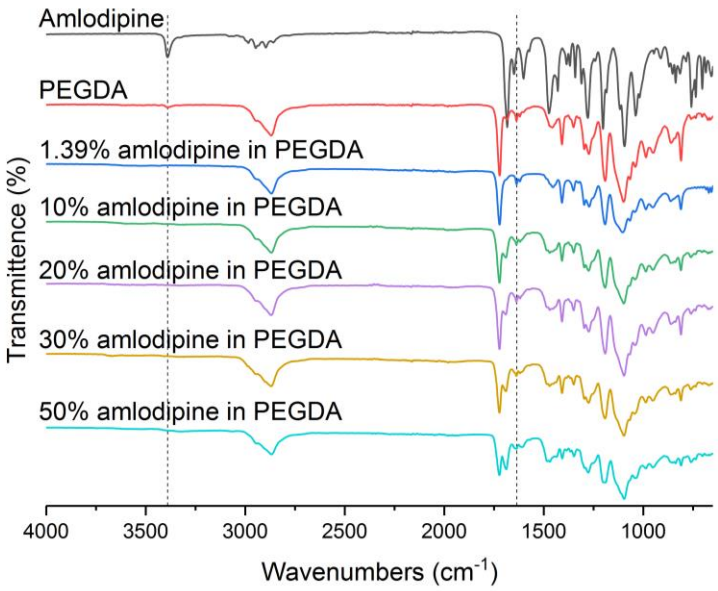

Fig~~ure~~ 6. FTIR spectra of amlodipine, PEGDA and mixtures of amlodipine-PEGDA.

NMR spectroscopy was performed to confirm the reaction between amlodipine and PEGDA. As the polyprintlets were designed to deliver a low-dose combination therapy, the photocrosslinkable monomer PEGDA was used in a large excess when compared with amlodipine (1.39 % w/w). The use of this formulation for NMR study, however, did not allow the observation of drug peaks. As such, the characteristic peaks of the combination of amlodipine to PEGDA were not detected due to the predominant signals of the distinct PEGDA peaks. Consequently, the molar ratio of amlodipine to PEGDA was increased to 2:1 for the ease in amlodipine peak detection and the covalent bond between amlodipine and PEGDA respectively. Fig. 7 shows the 1H NMR spectra of amlodipine, PEGDA and amlodipine-PEGDA mixture and Supplementary Figure A shows the 13C NMR spectra of amlodipine-PEGDA

Formatted: No underline

Formatted: Left

mixture. 2D NMR experiments, Heteronuclear Single Quantum Correlation (HSQC) (Supplementary Figure Bi) and Heteronuclear Multiple-Bond Correlation (HMBC) (Supplementary Figure Bii) facilitated the full assignment of the 1H and 13C NMR spectrum (Fig. 7 and Supplementary Figure A respectively). Each characteristic peak of PEGDA and amlodipine was detected in both 1D spectrum. However, an additional set of signals at 4.16, 3.62, 2.84 and 2.51 ppm (peaks labelled in green) was detected in the 1H NMR spectrum which were assigned to the methylene groups of PEGDA after interacting with amlodipine. Additionally, the intensity of the signals of the diacrylate group at 6.34, 6.20 and 5.91 ppm were much lower than expected from a molar ratio of amlodipine to PEGDA of 2:1.~~NMR spectroscopy was performed to confirm the reaction between amlodipine and PEGDA. As the polyprintlets were designed to deliver a low-dose combination therapy, the photocrosslinkable monomer PEGDA was used in a large excess when compared with amlodipine (1.39% w/w). The use of this formulation for NMR study, however, did not allow the observation of drug peaks. As such, the characteristic peaks of the combination of amlodipine to PEGDA were not detected due to the predominant signals of the distinct PEGDA peaks. Consequently, the molar ratio of amlodipine to PEGDA was increased to 2:1 for the ease in amlodipine peak detection and the covalent bond between amlodipine and PEGDA respectively. Figure 7 shows the ^{1}H NMR spectra of amlodipine, PEGDA and amlodipine-PEGDA mixture and Supplementary Figure A shows the ^{13}C NMR spectra of amlodipine-PEGDA mixture. 2D NMR experiments, Heteronuclear Single Quantum Correlation (HSQC) (Supplementary Figure Bi) and Heteronuclear Multiple-Bond Correlation (HMBC) (Supplementary Figure Bii) facilitated the full assignment of the ^{1}H and ^{13}C NMR spectrum (Figure 7 and Supplementary Figure A respectively). Each characteristic peak of PEGDA and amlodipine was detected in both 1D spectrum. However, an additional set of signals at 4.16, 3.62, 2.84 and 2.51 ppm (peaks labelled in green) was detected in the ^{1}H NMR spectrum which were assigned to the methylene groups of PEGDA after interacting with amlodipine. Additionally, the intensity of the signals of the diacrylate group at 6.34, 6.20 and 5.91 ppm were much lower than expected from a molar ratio of amlodipine to PEGDA of 2:1.~~

When compared with the spectra of amlodipine and PEGDA, the integral peak areas for the -NH- group of amlodipine and CH2=CH- of PEGDA were found to be only 0.83 and 0.10 in the amlodipine-PEGDA mixture. In other words, a ratio of amlodipine to PEGDA of 2:0.24 was calculated, thus indicating a loss of approximately 80 % of PEGDA due to its reaction with amlodipine. It is proposed that the primary amine of amlodipine and the diacrylate of PEGDA could undergo a Michael addition in mild conditions without the use of catalysts or solvents [40]. The proton at the position 27 has only three carbon correlations in the HMBC spectrum (Supplementary Figure A) indicating the formation of a secondary amine via the single functionalisation of the primary amine with PEGDA. Akyol et al. described the synthesis of novel poly(beta amino ester) macromonomers through Michael addition of various diacrylates including PEGDA and a phosphonate that contains primary amine, as well as propyl amine [41]. In their 1H-NMR spectra, a change of peaks was observed due to methylene groups attaching to a carbonyl group, nitrogen and oxygen. In addition, in the article where an example was given for a diacrylate and an amine, the NMR results illustrated the disappearance of the amino protons as well as the weak intensity of the acrylate peaks after they were interacting with each other [42].~~When compared with the spectra of amlodipine and PEGDA, the integral peak areas for the -NH- group of amlodipine and CH_2=CH- of PEGDA were found to be only 0.83 and 0.10 in the amlodipine-PEGDA mixture. In other words, a ratio of amlodipine to PEGDA of 2:0.24 was calculated, thus indicating a loss of approximately 80% of PEGDA due to its reaction with amlodipine. It is proposed that the primary amine of amlodipine and the diacrylate of PEGDA could undergo a Michael addition in mild conditions without the use of catalysts or solvents [1]. The proton at the position 27 has only three carbon correlations in the HMBC spectrum (Supplementary Figure A) indicating the formation of a secondary amine via the single functionalisation of the primary amine with PEGDA. Akyol *et al.* described the synthesis of novel poly(beta amino ester) macromonomers through Michael addition of various diacrylates including PEGDA and a phosphonate that contains primary amine, as well as propyl~~

~~amine [2]. In their 1H-NMR spectra, a change of peaks was observed due to methylene groups attaching to a carbonyl group, nitrogen and oxygen. In addition, in the article where an example was given for a diacrylate and an amine, the NMR results illustrated the disappearance of the amino protons as well as the weak intensity of the acrylate peaks after they were interacting with each other [3].~~

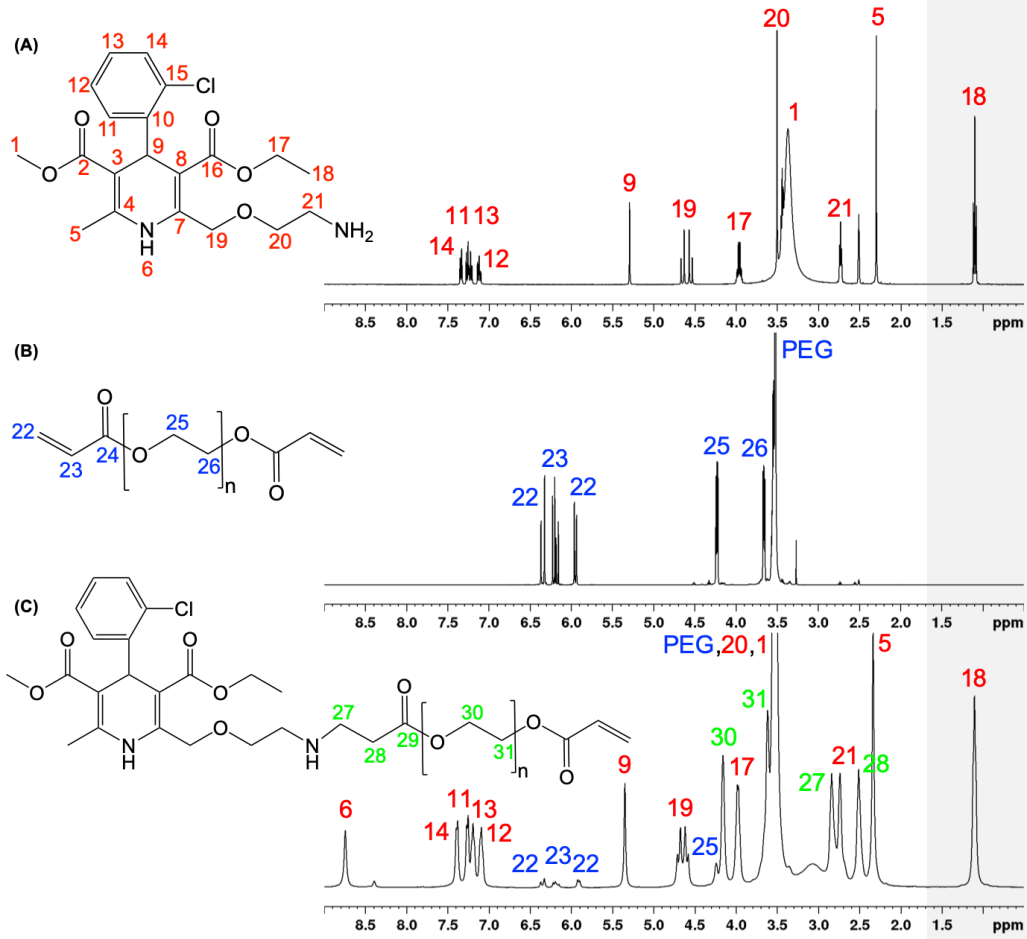

Fig~~ure~~ 7. ^{1}H NMR spectra (DMSO-d6) of (A) amlodipine, (B) PEGDA and (C) amlodipine-PEGDA mixture.

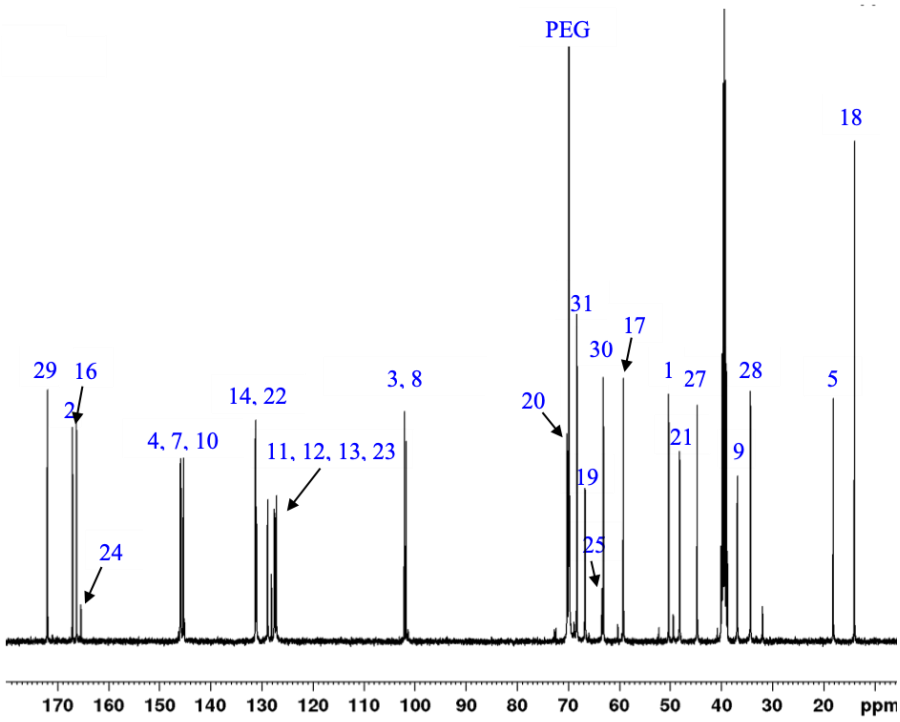

Supplementary Figure A. ^{13}C NMR spectrum (DMSO-d6) of amlodipine-PEGDA mixture.

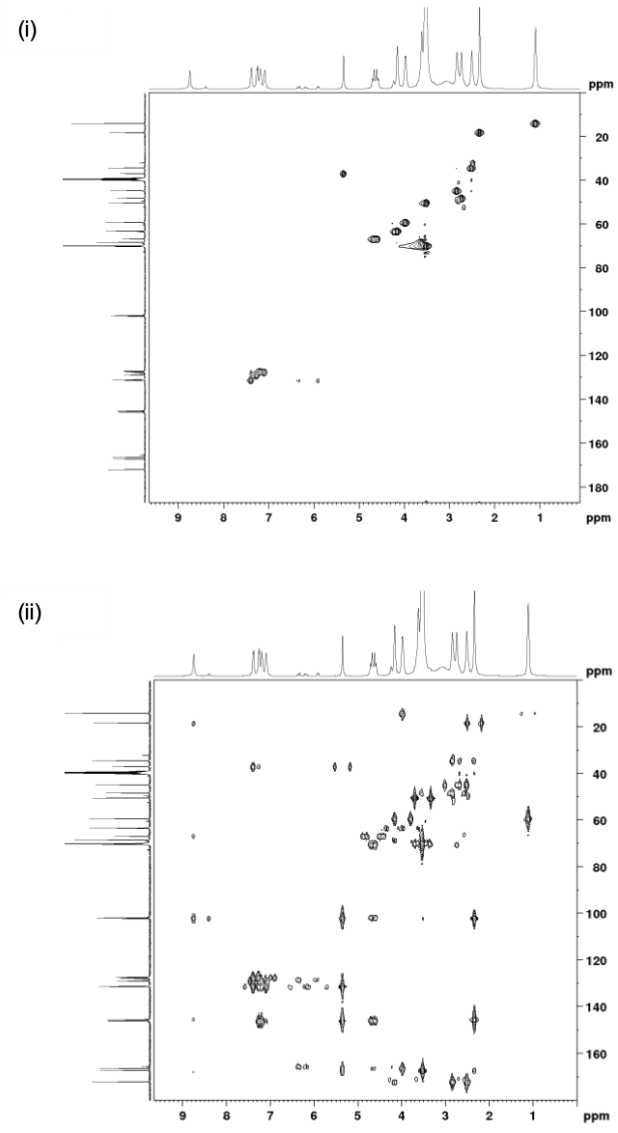

Supplementary Figure B. HSQC (i) and HMBC (ii) of amlodipine-PEGDA mixture in (DMSO-d6).

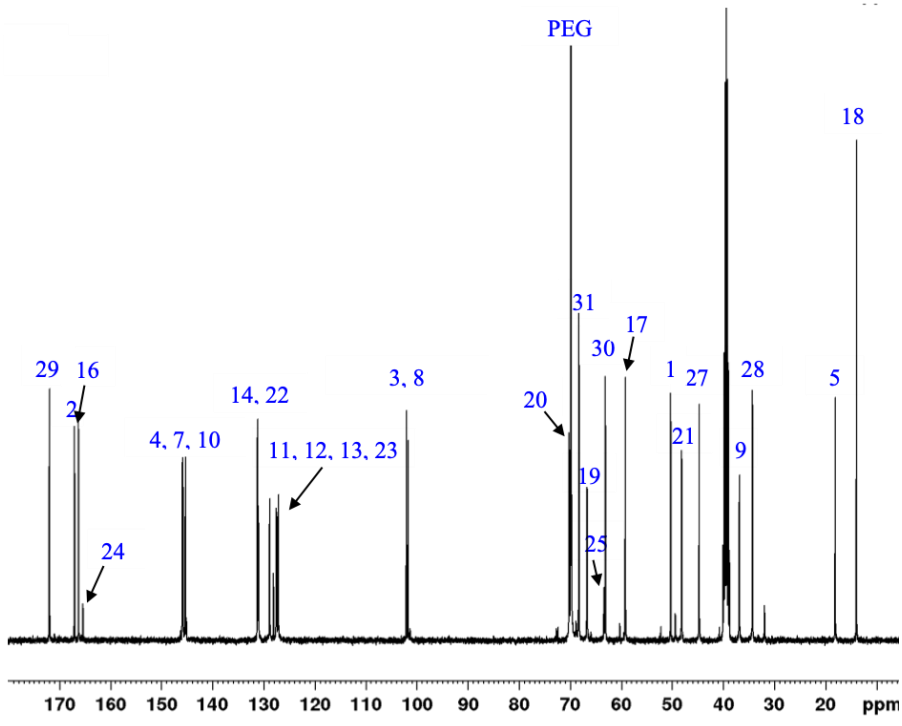

Supplementary Figure A. ^{13}C NMR spectrum (DMSO-d6) of amlodipine-PEGDA mixture.

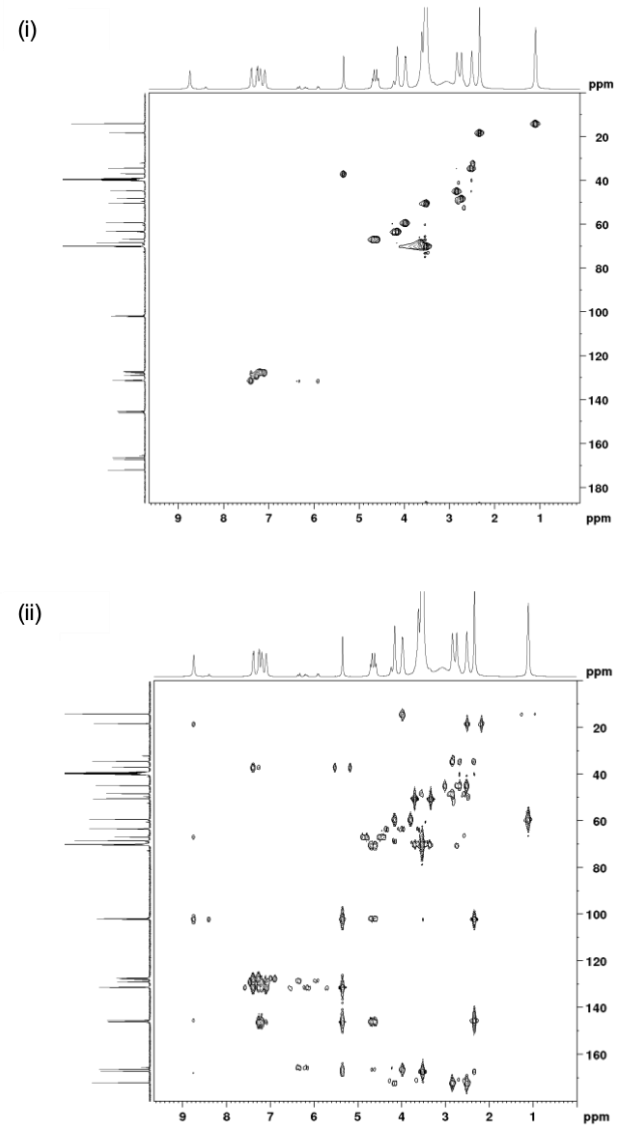

~~**Supplementary Figure B.** HSQC (i) and HMBC (ii) of amlodipine-PEGDA mixture in (DMSO-d6).~~

The SLA 3D printed polyprintlets were tested in the dynamic in vitro dissolution model that mimics the physiological conditions of the gastrointestinal tract. The drug release of atenolol, hydrochlorothiazide and irbesartan from both formulations commenced in the gastric phase and continued in the intestinal phase over a period of 24 h (Fig. 8). The polyprintlets were designed and formulated to evaluate the effect of geometry on the dissolution profiles. Over 75 % of atenolol was released in the first 120 min in Type 1 polyprintlets while 55 % drug release was achieved in the Type 2 polyprintlets in the same time. This coincided with the fact that atenolol was located on the outer layer in the Type 1 polyprintlets where surface area to volume ratio was higher than where it was in the Type 2 polyprintlets (inner layer) [43]. For hydrochlorothiazide and irbesartan, minimal changes in drug release were observed on the different surface to volume ratio of Types 1 and 2 polyprintlet. On the other hand, it was observed that atenolol was the only formulation to reach 100 % drug release in both polyprintlets while 48 % and 17 % of hydrochlorothiazide and irbesartan were released in total after 24 h. This was attributed mainly to their poor aqueous solubilities (0.70 mg/mL for hydrochlorothiazide and 0.00884 mg/mL for irbesartan) which consequently affect the drug dissolution rates from the polymeric matrix [44,45]. No release of amlodipine was detected in any type of polyprintlet which confirm the incompatibility of the drug via its reaction with PEGDA.

Crucially, undesirable reactions between the photoreactive monomer and the API should be avoided when using the SLA 3D printing approach in drug delivery, otherwise the active drug molecule could undergo possible degradation or iteration which can consequently deplete therapeutic effects. Previously, studies involving SLA 3D printing of oral dosage forms have demonstrated at least more than 90 % of drug contents in the printed tablets suggesting the absence of drug-photopolymer reactions [24,32]. A recent article that utilised the DLP 3D printing technology to fabricate oral tablets also employed FTIR to assess possible drug-polymer reactions. No detectable chemical reactions, however, were found in the oral formulations [25]. This could be due to the study design of proof of concept studies; researchers tend to select common drugs such as paracetamol, 4-aminosalicylic acid and

Formatted: Justified

theophylline to demonstrate the feasibility of using SLA 3D printing for printing drug-loaded tablets. Herein, however, we report that the reaction between drug and polymer could be possibly due to a Michael addition reaction under a solvent-free and catalyst-free conditions. This therefore may represent a limitation for the advancement of the SLA 3D printing technology in the development of oral dosage forms. Michael addition is a versatile polymer synthesis reaction that allows the biocompatible preparation of growth polymers including poly(amido amines), poly(amino esters) and poly(ester sulfides) [40]. Beyond primary amines, nucleophiles such as secondary amines, thiols and phosphines could perform as Michael donors to undergo Michael addition with numerous Michael acceptors including ester acrylates and acrylamides, for example [46].

Formatted: Justified

Active compounds which could serve as a Michael donor can react with a Michael acceptor (in this case the PEGDA or other monomers with diacrylate groups) even during the physical mixing procedure. To resolve this issue, other biocompatible photocrosslinkable monomers without acrylate groups should be considered to replace PEGDA. Alternative novel biomaterials have recently been developed for photopolymerisation-based 3D printing like alkyne carbonate based monomers which showed considerably lower cytotoxicity and higher conversion rates when compared with methacrylates [30]. Moreover, mixtures of poly(propylene fumarate) (PPF)/diethyl fumarate (DEF) [47] and vegetable oil-derived epoxy monomers [48] have also been exploited as photopolymerisable materials for SLA 3D printing.

~~The SLA 3D printed polyprintlets were tested in the dynamic *in vitro* dissolution model that mimics the physiological conditions of the gastrointestinal tract. The drug release of atenolol, hydrochlorothiazide and irbesartan from both formulations commenced in the gastric phase and continued in the intestinal phase over a period of 24 h (Figure 8). The polyprintlets were designed and formulated to evaluate the effect of geometry on the dissolution profiles. Over 75% of atenolol was released in the first 120 min in Type 1 polyprintlets while 55% drug release was achieved in the Type 2 polyprintlets in the same time. This coincided with the fact that~~

~~atenolol was located on the outer layer in the Type 1 polyprintlets where surface area to volume ratio was higher than where it was in the Type 2 polyprintlets (inner layer) [1]. For hydrochlorothiazide and irbesartan, minimal changes in drug release were observed on the different surface to volume ratio of Types 1 and 2 polyprintlet. On the other hand, it was observed that atenolol was the only formulation to reach 100% drug release in both polyprintlets while 48% and 17% of hydrochlorothiazide and irbesartan were released in total after 24 hr. This was attributed mainly to their poor aqueous solubilities (0.70 mg/mL for hydrochlorothiazide and 0.00884 mg/mL for irbesartan) which consequently affect the drug dissolution rates from the polymeric matrix [2, 3]. No release of amlodipine was detected in any type of polyprintlet which confirm the incompatibility of the drug via its reaction with PEGDA.~~

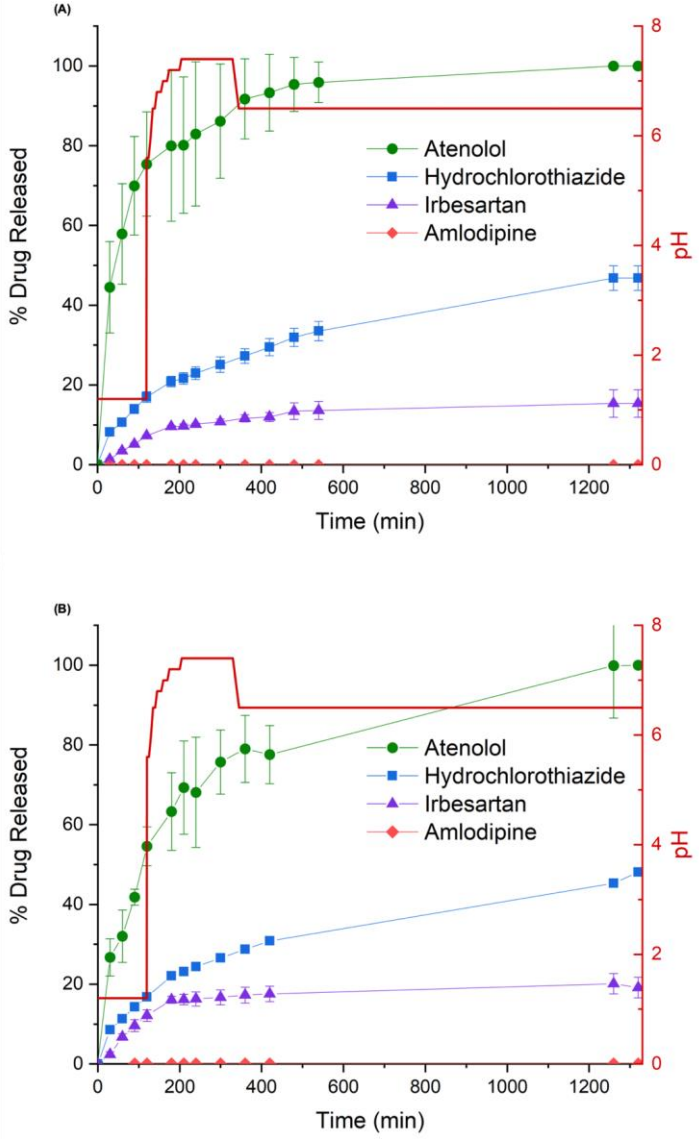

Fig~~ure~~ 8. Drug dissolution profiles from SLA 3D printed Type 1 (A) and Type 2 (B) polyprintlets. Red line shows the pH values of the dissolution media.

~~Crucially, undesirable reactions between the photoreactive monomer and the API should be avoided when using the SLA 3DP approach in drug delivery, otherwise the active drug molecule could undergo possible degradation or iteration which can consequently deplete therapeutic effects. Previously, studies involving SLA 3DP of oral dosage forms have demonstrated at least more than 90% of drug contents in the printed tablets suggesting the absence of drug-photopolymer reactions [1, 2]. A recent article that utilised the DLP 3DP technology to fabricate oral tablets also employed FTIR to assess possible drug-polymer reactions. No detectable chemical reactions, however, were found in the oral formulations [3]. This could be due to the study design of proof of concept studies; researchers tend to select common drugs such as paracetamol, 4-aminosalicylic acid and theophylline to demonstrate the feasibility of using SLA 3DP for printing drug-loaded tablets. Herein, however, we report that the reaction between drug and polymer could be possibly due to a Michael addition reaction under a solvent-free and catalyst-free conditions. This therefore may represent a limitation for the advancement of the SLA 3DP technology in the development of oral dosage forms. Michael addition is a versatile polymer synthesis reaction that allows the biocompatible preparation of growth polymers including poly(amido amines), poly(amino esters) and poly(ester sulfides) [4]. Beyond primary amines, nucleophiles such as secondary amines, thiols and phosphines could perform as Michael donors to undergo Michael addition with numerous Michael acceptors including ester acrylates and acrylamides, for example [5].~~

~~Active compounds which could serve as a Michael donor can react with a Michael acceptor (in this case the PEGDA or other monomers with diacrylate groups) even during the physical mixing procedure. To resolve this issue, other biocompatible photocrosslinkable monomers without acrylate groups should be considered to replace PEGDA. Alternative novel biomaterials have recently been developed for photopolymerisation-based 3DP like alkyne carbonate based monomers which showed considerably lower cytotoxicity and higher conversion rates when compared with methacrylates [6]. Moreover, mixtures of poly(propylene~~

~~fumarate) (PPF)/diethyl fumarate (DEF) [7] and vegetable oil-derived epoxy monomers [8] have also been exploited as photopolymerisable materials for SLA 3DP.~~

4. Conclusion

~~In this study, we successfully report the fabrication of a multi-layer antihypertensive polyprintlet that could potentially deliver a low-dose combination therapy utilising a novel SLA 3DP approach. Notably, reactions between photocrosslinkable monomers (PEGDA) and one of the drugs (amlodipine) were demonstrated and confirmed using FTIR and NMR spectroscopy. To the best of our knowledge, the findings from our case study was the first to describe the unexpected drug-polymer reactions in 3DP. As such, this highlights the need to screen for photoreactive monomers to ensure the compatibility of drug-loaded oral dosage forms manufactured by SLA. This work presents the vast opportunities and consequently the challenges that need to be addressed towards the advancement of novel and versatile photocurable biomaterials in 3DP for drug delivery.~~

In this study, we successfully report the fabrication of a multi-layer antihypertensive polyprintlet that could potentially deliver a low-dose combination therapy utilising a novel SLA 3D printing approach. Notably, reactions between photocrosslinkable monomers (PEGDA) and one of the drugs (amlodipine) were demonstrated and confirmed using FTIR and NMR spectroscopy. To the best of our knowledge, the findings from our case study was the first to describe the unexpected drug-polymer reactions in 3D printing. As such, this highlights the need to screen for photoreactive monomers to ensure the compatibility of drug-loaded oral dosage forms manufactured by SLA. This work presents the vast opportunities and consequently the challenges that need to be addressed towards the advancement of novel and versatile photocurable biomaterials in 3D printing for drug delivery.

CRediT authorship contribution statement

Xiaoyan Xu: Conceptualization, Methodology, Software, Validation, Formal analysis, Investigation, Resources, Data curation, Writing - original draft, Writing - review & editing. Pamela Robles-Martinez: Conceptualization, Methodology, Software, Validation, Formal

Formatted: Font: Bold

analysis, Investigation, Resources, Data curation, Writing – review & editing, Visualization. Christine M. Madla: Conceptualization, Methodology, Resources, Writing - review & editing. Fanny Joubert: Conceptualization, Methodology, Software, Validation, Formal analysis, Investigation, Data curation, Writing - review & editing. Alvaro Goyanes: Conceptualization, Methodology, Resources, Writing – review & editing, Supervision, Project administration. Abdul W. Basit: Conceptualization, Methodology, Writing - review & editing, Supervision, Project administration. Simon Gaisford: Conceptualization, Methodology, Writing - review & editing, Supervision, Project administration.

Declaration of Competing Interest

The authors declare no conflict of interest.

Acknowledgement

This research was funded by the Engineering and Physical Sciences Research Council (EPSRC) UK, grant number EP/L01646X.

Appendix A. Supplementary data

Supplementary material related to this article can be found, in the online version, at https://doi.org/10.1016/j.addma.2020.101071.

Formatted: Font: Bold

Formatted: Font: Not Bold

Formatted: Font: Not Bold

Field Code Changed

Formatted: Hyperlink, Font: (Default) +Body (DengXian), 12 pt, Not Bold, English (United States)

Formatted: Font: Not Bold

References

[1] S.J. Trenfield, A. Awad, C.M. Madla, G.B. Hatton, J. Firth, A. Goyanes, S. Gaisford, A.W. Basit, Shaping the future: recent advances of 3D printing in drug delivery and healthcare, Expert Opin. Drug Deliv. 16 (10) (2019) 1081–1094.

[2] S.C. Joshi, A.A. Sheikh, 3D printing in aerospace and its long-term sustainability, Virtual Phys. Prototyp. 10 (4) (2015) 175–185.

[3] J. Sun, W. Zhou, L. Yan, D. Huang, L.-y. Lin, Extrusion-based food printing for digitalized food design and nutrition control, J. Food Eng. 220 (2018) 1–11.

[4] M. Wehner, R.L. Truby, D.J. Fitzgerald, B. Mosadegh, G.M. Whitesides, J.A. Lewis, R.J. Wood, An integrated design and fabrication strategy for entirely soft, autonomous robots, Nature 536 (7617) (2016) 451–455.

[5] W. Peng, P. Datta, B. Ayan, V. Ozbolat, D. Sosnoski, I.T. Ozbolat, 3D bioprinting for drug discovery and development in pharmaceutics, Acta Biomater. 57 (2017) 26–46.

[6] Aprecia Pharmaceuticals, FDA approves the first 3D printed drug product, https://www.aprecia.com/pdf/2015_08_03_Spritam_FDA_Approval_Press_Release.pdf, last accessed 09-2018 (2015).

[7] F. Fina, C.M. Madla, A. Goyanes, J. Zhang, S. Gaisford, A.W. Basit, Fabricating 3D printed orally disintegrating printlets using selective laser sintering, Int. J. Pharm. 541 (1-2) (2018) 101–107.

[8] P.R. Martinez, A. Goyanes, A.W. Basit, S. Gaisford, Influence of geometry on the drug release profiles of stereolithographic (SLA) 3D-printed tablets, AAPS PharmSciTech 19 (8) (2018) 3355–3361.

[9] A. Goyanes, M. Scarpa, M. Kamlow, S. Gaisford, A.W. Basit, M. Orlu, Patient acceptability of 3D printed medicines, Int. J. Pharm. 530 (1) (2017) 71–78.

[10] A. Goyanes, N. Allahham, S.J. Trenfield, E. Stoyanov, S. Gasiford, A.W. Basit, Direct powder extrusion 3D printing: fabrication of drug products using a novel, single-step process, Int. J. Pharm. (2019) 118471.

[11] F. Fina, A. Goyanes, C.M. Madla, A. Awad, S.J. Trenfield, J.M. Kuek, P. Patel, S. Gaisford, A.W. Basit, 3D printing of drug-loaded gyroid lattices using selective laser sintering, Int. J. Pharm. 547 (1-2) (2018) 44–52.

[12] A. Isreb, K. Baj, M. Wojsz, M. Isreb, M. Peak, M.A. Alhnan, 3D printed oral theophylline doses with innovative 'radiator-like' design: impact of polyethylene oxide (PEO) molecular weight, Int. J. Pharm. 564 (2019) 98–105.

[13] M. Sadia, B. Arafat, W. Ahmed, R.T. Forbes, M.A. Alhnan, Channelled tablets: an innovative approach to accelerating drug release from 3D printed tablets, J. Control. Release 269 (2018) 355–363.

[14] N. Genina, J.P. Boetker, S. Colombo, N. Harmankaya, J. Rantanen, A. Bohr, Antituberculosis drug combination for controlled oral delivery using 3D printed compartmental dosage forms: from drug product design to in vivo testing, J. Control. Release 268 (2017) 40–48.

[15] B.C. Pereira, A. Isreb, R.T. Forbes, F. Dores, R. Habashy, J.-B. Petit, M.A. Alhnan, E.F. Oga, 'Temporary Plasticiser': a novel solution to fabricate 3D printed patientcentred cardiovascular 'Polypill' architectures, Eur. J. Pharm. Biopharm. 135 (2019) 94–103.

[16] A. Maroni, A. Melocchi, F. Parietti, A. Foppoli, L. Zema, A. Gazzaniga, 3D printed multi-compartment capsular devices for two-pulse oral drug delivery, J. Control. Release 268 (2017) 10–18.

[17] A. Goyanes, A. Fernández-Ferreiro, A. Majeed, N. Gomez-Lado, A. Awad, A. Luaces-Rodríguez, S. Gaisford, P. Aguiar, A.W. Basit, PET/CT imaging of 3D printed devices in the gastrointestinal tract of rodents, Int. J. Pharm. 536 (1) (2018) 158–164.

[18] D.M. Smith, Y. Kapoor, G.R. Klinzing, A.T. Procopio, Pharmaceutical 3D printing: design and qualification of a single step print and fill capsule, Int. J. Pharm. 544 (1) (2018) 21–30.

[19] A. Goyanes, C.M. Madla, A. Umerji, G. Duran Piñeiro, J.M. Giraldez Montero, M.J. Lamas Diaz, M. Gonzalez Barcia, F. Taherali, P. Sánchez-Pintos, M.-L. Couce, S. Gaisford, A.W. Basit, Automated therapy preparation of isoleucine formulations using 3D printing for the treatment of MSUD: first single-centre, prospective, crossover study in patients, Int. J. Pharm. 567 (2019)

118497.

[20] S.A. Khaled, J.C. Burley, M.R. Alexander, J. Yang, C.J. Roberts, 3D printing of five-in-one dose combination polypill with defined immediate and sustained release profiles, J. Control. Release 217 (2015) 308–314.

[21] A. Goyanes, J. Wang, A. Buanz, R. Martínez-Pacheco, R. Telford, S. Gaisford, A.W. Basit, 3D printing of medicines: engineering novel oral devices with unique design and drug release characteristics, Mol. Pharm. 12 (11) (2015) 4077–4084.

[22] A. Awad, F. Fina, S.J. Trenfield, P. Patel, A. Goyanes, S. Gaisford, A.W. Basit, 3D printed pellets (Miniprintlets): a novel, multi-drug, controlled release platform technology, Pharmaceutics 11 (4) (2019) 148.

[23] A. Awad, S.J. Trenfield, A. Goyanes, S. Gaisford, A.W. Basit, Reshaping drug development using 3D printing, Drug Discov. Today 23 (8) (2018) 1547–1555.

[24] J. Wang, A. Goyanes, S. Gaisford, A.W. Basit, Stereolithographic (SLA) 3D printing of oral modified-release dosage forms, Int. J. Pharm. 503 (1-2) (2016) 207–212.

[25] H. Kadry, S. Wadnap, C. Xu, F. Ahsan, Digital light processing (DLP) 3D-printing technology and photoreactive polymers in fabrication of modified-release tablets, Eur. J. Pharm. Sci. 135 (2019) 60–67.

[26] C.J. Bloomquist, M.B. Mecham, M.D. Paradzinsky, R. Janusziewicz, S.B. Warner, J.C. Luft, S.J. Mecham, A.Z. Wang, J.M. DeSimone, Controlling release from 3D printed medical devices using CLIP and drug-loaded liquid resins, J. Control. Release 278 (2018) 9–23.

[27] G. Kollamaram, D.M. Croker, G.M. Walker, A. Goyanes, A.W. Basit, S. Gaisford, Low temperature fused deposition modeling (FDM) 3D printing of thermolabile drugs, Int. J. Pharm. 545 (1-2) (2018) 144–152.

[28] A. Goyanes, U. Det-Amornrat, J. Wang, A.W. Basit, S. Gaisford, 3D scanning and 3D printing as innovative technologies for fabricating personalized topical drug delivery systems, J. Control. Release 234 (2016) 41–48.

[29] A. Bagheri, J. Jin, Photopolymerization in 3D Printing, ACS Appl. Polym. Mater. 1 (4) (2019) 593–611.

[30] A. Oesterreicher, J. Wiener, M. Roth, A. Moser, R. Gmeiner, M. Edler, G. Pinter, T. Griesser, Tough and degradable photopolymers derived from alkyne monomers for 3D printing of biomedical materials, Polym. Chem. 7 (32) (2016) 5169–5180.

[31] P.R. Martinez, A. Goyanes, A.W. Basit, S. Gaisford, Fabrication of drug-loaded hydrogels with stereolithographic 3D printing, Int. J. Pharm. 532 (1) (2017) 313–317.

[32] P. Robles-Martinez, X. Xu, S.J. Trenfield, A. Awad, A. Goyanes, R. Telford, A.W. Basit, S. Gaisford, 3D printing of a multi-layered polypill containing six drugs using a novel stereolithographic method, Pharmaceutics 11 (6) (2019) 274.

[33] S.J. Trenfield, A. Awad, A. Goyanes, S. Gaisford, A.W. Basit, 3D printing pharmaceuticals: drug development to frontline care, Trends Pharmacol. Sci. 39 (5) (2018) 440–451.

[34] R.L. Maher, J. Hanlon, E.R. Hajjar, Clinical consequences of polypharmacy in elderly, Expert Opin. Drug Saf. 13 (1) (2014) 57–65.

[35] N.J. Wald, M.R. Law, A strategy to reduce cardiovascular disease by more than 80%, BMJ 326 (7404) (2003) 1419.

[36] C.K. Chow, J. Thakkar, A. Bennett, G. Hillis, M. Burke, T. Usherwood, K. Vo, K. Rogers, E. Atkins, R. Webster, M. Chou, H.-M. Dehbi, A. Salam, A. Patel, B. Neal, D. Peiris, H. Krum, J. Chalmers, M. Nelson, C.M. Reid, M. Woodward, S. Hilmer, S. Thom, A. Rodgers, Quarter-dose quadruple combination therapy for initial treatment of hypertension: placebo-controlled, crossover, randomised trial and systematic review, Lancet 389 (10073) (2017) 1035–1042.

[37] H.M. Fadda, A.W. Basit, Dissolution of pH responsive formulations in media resembling intestinal fluids: bicarbonate versus phosphate buffers, J. Drug Deliv. Sci. Technol. 15 (4) (2005) 273–279.

[38] A. Goyanes, G.B. Hatton, H.A. Merchant, A.W. Basit, Gastrointestinal release behaviour of modified-release drug products: Dynamic dissolution testing of mesalazine formulations, Int. J. Pharm. 484 (1-2) (2015) 103–108.

[39] H.A. Merchant, A. Goyanes, N. Parashar, A.W. Basit, Predicting the gastrointestinal behaviour of modified-release products: utility of a novel dynamic dissolution test apparatus involving the use of bicarbonate buffers, Int. J. Pharm. 475 (1-2) (2014) 585–591.

[40] E.S. Read, K.L. Thompson, S.P. Armes, Synthesis of well-defined primary aminebased homopolymers and block copolymers and their Michael addition reactions with acrylates and acrylamides, Polym. Chem. 1 (2) (2010) 221–230.

[41] E. Akyol, M. Tatliyuz, F. Demir Duman, M.N. Guven, H.Y. Acar, D. Avci, Phosphonate-functionalized poly(beta-amino ester) macromers as potential biomaterials, J. Biomed. Mater. Res. A 106 (5) (2018) 1390–1399.

[42] D.G. Anderson, C.A. Tweedie, N. Hossain, S.M. Navarro, D.M. Brey, K.J. Van Vliet, R. Langer, J.A. Burdick, A combinatorial library of photocrosslinkable and degradable materials, Adv. Mater. 18 (19) (2006) 2614–2618.

[43] A. Goyanes, P. Robles Martinez, A. Buanz, A.W. Basit, S. Gaisford, Effect of geometry on drug release from 3D printed tablets, Int. J. Pharm. 494 (2) (2015) 657–663.

[44] J. Patel, A. Patel, M. Raval, N. Sheth, Formulation and development of a self-nanoemulsifying drug delivery system of irbesartan, J. Adv. Pharm. Technol. Res. 2 (1) (2011) 9.

[45] A. Khan, Z. Iqbal, Y. Shah, L. Ahmad, Z. Ullah, A. Ullah, Enhancement of dissolution rate of class II drugs (Hydrochlorothiazide); a comparative study of the two novel approaches; solid dispersion and liqui-solid techniques, Saudi Pharm. J. 23 (6) (2015) 650–657.

[46] B.D. Mather, K. Viswanathan, K.M. Miller, T.E. Long, Michael addition reactions in macromolecular design for emerging technologies, Prog. Polym. Sci. 31 (5) (2006) 487–531.

[47] Y. Lu, S.N. Mantha, D.C. Crowder, S. Chinchilla, K.N. Shah, Y.H. Yun, R.B. Wicker, J.W. Choi, Microstereolithography and characterization of poly(propylene fumarate)-based drug-loaded microneedle arrays, Biofabrication 7 (4) (2015) 045001.

[48] D.S. Branciforti, S. Lazzaroni, C. Milanese, M. Castiglioni, F. Auricchio, D. Pasini, D. Dondi, Visible light 3D printing with epoxidized vegetable oils, Addit. Manuf. 25 (2019) 317–324.

Formatted: Font: Not Bold

~~References~~

~~[1] J. Wang, A. Goyanes, S. Gaisford, A.W. Basit, Stereolithographic (SLA) 3D printing of oral modified-release dosage forms, Int J Pharm 503(1-2) (2016) 207-12.~~

~~[2] P. Robles-Martinez, X. Xu, S.J. Trenfield, A. Awad, A. Goyanes, R. Telford, A.W. Basit, S. Gaisford, 3D Printing of a Multi-Layered Polypill Containing Six Drugs Using a Novel~~

Stereolithographic Method, Pharmaceutics 11(6) (2019) 274.

[3] H. Kadry, S. Wadnap, C. Xu, F. Ahsan, Digital light processing (DLP) 3D-printing technology and photoreactive polymers in fabrication of modified-release tablets, Eur J Pharm Sci 135 (2019) 60-67.

[4] E.S. Read, K.L. Thompson, S.P. Armes, Synthesis of well-defined primary amine-based homopolymers and block copolymers and their Michael addition reactions with acrylates and acrylamides, Polymer Chemistry 1(2) (2010) 221-230.

[5] B.D. Mather, K. Viswanathan, K.M. Miller, T.E. Long, Michael addition reactions in macromolecular design for emerging technologies, Progress in Polymer Science 31(5) (2006) 487-531.

[6] A. Oesterreicher, J. Wiener, M. Roth, A. Moser, R. Gmeiner, M. Edler, G. Pinter, T. Griesser, Tough and degradable photopolymers derived from alkyne monomers for 3D printing of biomedical materials, Polymer Chemistry 7(32) (2016) 5169-5180.

[7] Y. Lu, S.N. Mantha, D.C. Crowder, S. Chinchilla, K.N. Shah, Y.H. Yun, R.B. Wicker, J.W. Choi, Microstereolithography and characterization of poly(propylene fumarate)-based drug-loaded microneedle arrays, Biofabrication 7(4) (2015) 045001.

[8] D.S. Branciforti, S. Lazzaroni, C. Milanese, M. Castiglioni, F. Auricchio, D. Pasini, D. Dondi, Visible-light 3D printing with epoxidized vegetable oils, Additive Manufacturing 25 (2019) 317-324.